PERGAMON

Atmospheric Environment 34 (2000) 1583–1590

ATMOSPHERIC ENVIRONMENT

www.elsevier.com/locate/atmosenv

A study on the distributions of the measured fluctuating wind velocity components

John Z. Yim*, Chun-Ren Chou, Wei-Po Huang

Department of Harbour & River Engineering, National Taiwan Ocean University, 2 Bee-Ning Road, 20224 Keelung, Taiwan

Received 13 April 1999; received in revised form 30 August 1999; accepted 30 August 1999

Abstract

Probability distributions of the three wind velocity components measured at a height of 26 m near the coast in Keelung, Taiwan were studied using statistical models found in the literature. Both the linear Gaussian distribution and a weakly nonlinear model were used. It is shown here that, for this specific site, the model based on the Gram–Charlier type A series expansions can be used to model all the three fluctuating velocity components more satisfactorily than the Gaussian model.

Keywords: Turbulent fluctuations; Probability distribution; Gaussian distribution; Gram–Charlier series expansions

1. Introduction

Winds are inevitably of turbulent nature. The fluctuating velocity components constitute the major characteristics of a turbulent wind field, which leads to enhanced momentum and mass transfer within the atmospheric boundary layer. Across the air-sea boundary layer, turbulent winds contribute the major portion of the energy and momentum exchange between the atmosphere and the ocean, which then dominates our local weather systems (Smith et al., 1992). Knowledge of the wind climate is important for a variety of reasons. In short terms, the statistical characteristics of the horizontal wind velocity components are vital for studying and modelling of the pollutant transport process (Weber, 1998). In long terms, the civil engineers may need to know the most probable extreme wind speed to design and construct their structures (Cook, 1985; Simiu and Scanlan, 1996).

It is generally assumed that the distributions of the horizontal wind components can be described through the Gaussian model. Weber (1998) used an isotropic Gaussian model (IGM) to describe the relation between the longitudinal and the lateral components of the horizontal wind vector. He found that the standard deviations of the horizontal velocity components, σ_v and σ_u, can be accurately estimated using this model. In passing, it should be noted that one of the basic assumptions that resulted in a normal distribution is that the phenomenon under consideration is the cumulative result of many independent influential factors (Thiebaux, 1994). In this respect, it seems hardly conceivable that the horizontal components of the local winds could satisfy this assumption.

Quite often, available wind data are in forms of 10 min mean speeds and directions. Wind data in this form can be used to study the long-term statistical properties but are not suitable for the present purpose. To study the fluctuating characteristics of a local wind field, continuously recorded data with a relatively high sampling rate are required. In 1998, an ultrasonic anemometer was installed on the roof of the Department of Harbour and River Engineering of National Taiwan Ocean University. Data recording started in May 1998 and continued to the present day. This paper summarizes some of the preliminary results.

In the following, we further divide this article into four sections. Section 2 contains a short description of the measuring site and the instrumentation. In Section 3, we briefly describe the models used in this study. The results

* Corresponding author. Fax: + 886-2-2463-3684.
E-mail address: b0052@ind.ntou.edu.tw (J.Z. Yim)

1352-2310/00/$ - see front matter
PII: S1352-2310(99)00414-8

of our analyses, together with discussions, will be presented in Section 4. It is shown there that the statistical distributions for all the three fluctuating wind components could be better described with the Gram–Charlier series expansions. A short conclusion in Section 5 then closes this paper.

2. The measuring site and instrumentation

2.1. The measuring site

The characteristics of a wind field can be influenced by factors such as the underlying topographical configurations, or the stratification of the atmosphere. The most predominant one among these factors is the topographic conditions, which are responsible for the roughness length and thus the velocity profile above. The measuring site of the present study is not ideal in that, the Institute building is located approximately 50 m away from the coast, and a small hill of approximately 150 m height is located some 150 m in front of the building. The 5-floor Institute building, together with a small water reservoir atop of it, is approximately 23 m high. As was shown by many researchers (e.g. Singh et al., 1994), building configurations have profound effects on the variations of the velocity components. In this respect, results presented in this paper cannot be considered representative of the natural atmosphere. However, since Taiwan is a mountainous island with the second densest population of the world, it was considered that, the geographical conditions of the present measuring site should be representative of those most frequently encountered in Taiwan. It is also hoped that, in long terms, statistical properties of the present measuring station could be compared and extrapolated to other measuring stations around the island. A schematic sketch showing the geographical location of the measuring site is given in Fig. 1.

The city Keelung is located in the northeastern part of Taiwan with one side facing the Pacific Ocean. Approximately nine months of a year, starting from September to May the next year, the city experiences relatively strong monsoon winds with the prevailing direction of NNE. In the rest of the months, especially in summer seasons, mild southwest winds are predominant. However, with occasional typhoon invasions in these months, the recorded extreme wind speeds can exceed 35 m s^{-1}. According to the records of the Central Weather Bureau (CWB) of ROC, in the 10-yr period from 1984 to 1994, only approximately 3.4% of the recorded wind speeds are in range from 13.9 to 17.1 m s^{-1}. It should be mentioned that in this statistics the extreme winds due to typhoon invasions are excluded. All these strong winds occurred during the winter seasons.

2.2. The instrumentation

A 3-D ultrasonic anemometer, type TJ-61B of the KAIJO Corporation, was mounted on a mast. As shown in Fig. 1, the 3 m mast is anchored on the roof of the building of the Department. The total height of the anemometer is 26 m above the ground. According to the manufacture specifications, wind speeds up to 60 m s^{-1} can be measured reliably by the anemometer. The resolution of the measurement is 0.005 m s^{-1}. Temperature can also be measured from -10 to 40° Celsius, with a resolution of 0.025°C. The positive x-axis of the anemometer is oriented toward the west and the positive y-axis toward the south, with the z-axis positive upwards. Variations of the three components of the wind speeds were recorded continuously. The sampling rate is 20 Hz. Changes of temperature were also recorded simultaneously, but these were not used here in this paper. Data recording started on 20 May 1998, and was stored in files separated by the hours of the day. An hourly data thus contains approximately 72,000 data points.

At first, we have used the whole data set of the 60 min records to determine the possible distributions of the three fluctuating velocity components. It was then decided that, data sets with such a long duration could violate the stationarity assumption, and results of the statistical inference may thus become questionable. We have further divided each of the 1 h data record into six 10 min interval sub-records. The mean values, as well as the turbulent fluctuations, of the velocity components were then recalculated, and the parameters for the statistical models were reestimated for each of the sub-intervals. All analyses were conducted on an IBM compatible personal computer with a Pentium II processor. Both the 60 and the 10 min results are presented in this paper.

3. Statistical models used

All data sets were first mean- and trend-removed (Bendat and Piersol, 1986). The fluctuating velocity components were normalized using their respective root-mean square (rms) values, $\hat{x}'_i = x'_i/x'_{i\mathrm{rms}}$, where $x'_i = (u', v', w')$. In the following, the hatch above the velocity components will be dropped for simplicity. Two statistical models were applied in this study to explore the possible distributions of the three fluctuating velocity components. The applied models are:

1. The normal or Gaussian distribution.

$$p(x, \mu, \sigma) = \frac{1}{\sigma\sqrt{2\pi}} \exp\left[-\frac{(x-\mu)^2}{2\sigma^2} \right], \tag{1}$$

where x denotes the normalized fluctuating components, $x = x'/x'_{\mathrm{rms}}$, with $x' = (u', v', w')$, μ is the mean, and σ is the standard deviation of the sample set. The

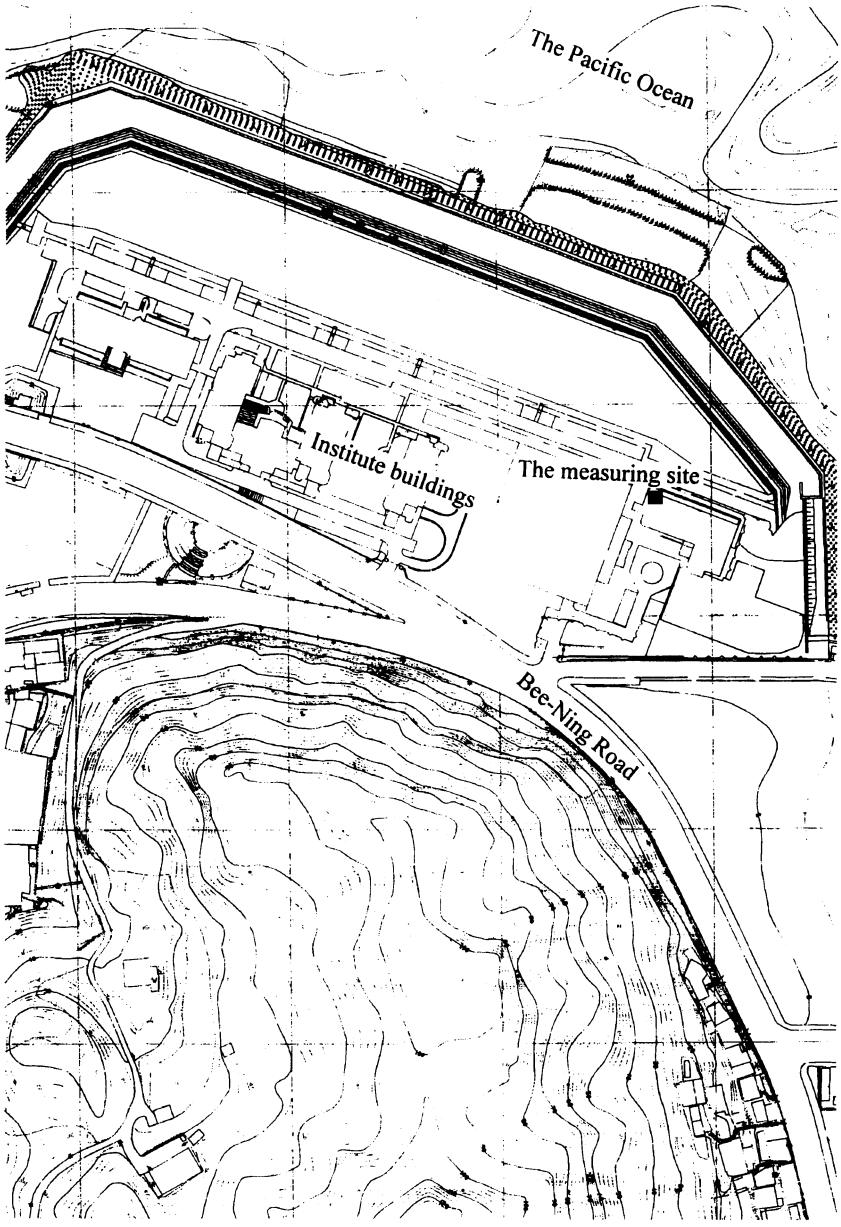

Fig. 1. Schematic geographical location of the measuring site.

mean value determines the location of the peak of the distribution, and is often called the location parameter. The standard deviation, σ, determines the spread of the curve, and is known as the scale parameter (Hahn and Shapiro, 1967).

2. The Edgeworth's type A of the Gram–Charlier series expansion (Ochi, 1992):

$$p(x) = \frac{1}{\sqrt{2\pi K_2}} \exp\left[-\frac{t^2}{2}\right]\left[1 + \frac{1}{6}\lambda_3 H_3 + \frac{1}{24}\lambda_4 H_4 + \frac{\lambda_5 H_5}{120} + \frac{(\lambda_6 + 10\lambda_3^2)}{720} H_6 + \frac{(\lambda_7 + 35\lambda_4\lambda_3)}{5040} H_7 + ..\right], \quad (2)$$

where x is the dimensionless fluctuations, and k_n the nth cumulant, and

$$t = \frac{x}{\sqrt{k_2}}, \quad (3)$$

$$\lambda_n = \frac{k_n}{(\sqrt{k_2})^n}, \tag{4}$$

H_n is the nth Hermit polynomial, with

$$H_3(t) = t^3 - 3t, \tag{5.1}$$

$$H_4(t) = t^4 - 6t^2 + 3, \tag{5.2}$$

$$H_5(t) = t^5 - 10t^3 + 15t. \tag{5.3}$$

Use of higher-order terms for the series does not necessarily guarantee a better result (Ochi, 1992). During the fit, all calculations of the series were therefore stopped at the fifth order.

Eq. (2) was derived by Longuet–Higgins (1963) using the so-called cumulant generating function. He showed that when the finite amplitude effects of water waves become important, the probability distribution of the surface fluctuations will deviate from normality and is then better described by this model. Huang and Long (1980) used wind–wave flume data to study the probability distribution of the water surface. They demonstrated that the Gram–Charlier series expansion could fit the skewed distribution of the surface elevations more adequately than the Gaussian model. It should be mentioned that occasionally, the Gram–Charlier series expansions may have negative values. This is the major drawback of the model when used as a probability function. Fortunately, our experiences have shown that this does not occur often, and even if the negative values do result, they are often small enough to be neglected.

χ^2 goodness-of-fit test were conducted for the Gaussian distribution. To evaluate the χ^2-test results, a prerequisite is the knowledge of the degrees of freedom of the underlying statistical model. Since the degrees of freedom depend on the parameters of the distribution, no χ^2 goodness-of-fit test could therefore be performed for the Gram–Charlier series. Furthermore, the χ^2-test is known not to be as stringent as other available tests. The fitted results were therefore further verified using the Kolmogorov–Smirnov test (Ochi, 1992).

As mentioned earlier, the measured horizontal wind velocity components are oriented in the north–south and east–west directions. Weber (1998) showed that the variances of these velocity components could be transformed into the instantaneous x- and y-components through the following relationships:

$$\bar{e} = \frac{1}{N}\sum_{i=1}^{N} e_i, \tag{6}$$

$$\bar{n} = \frac{1}{N}\sum_{i=1}^{N} n_i, \tag{7}$$

where e_i and n_i are, respectively, the measured east–west and south–north wind components, $\bar{e}$ and $\bar{n}$ are the mean wind speeds of the 10 min interval. A mean direction, $\bar{\theta}$, can be defined using these mean values:

$$\bar{\theta} = \tan^{-1}\left(\frac{\bar{n}}{\bar{e}}\right), \tag{8}$$

which is measured counterclockwise from the east–west direction. Weber further showed that the variances of the longitudinal and lateral wind components can be computed through the following equation:

$$\sigma_u^2 = \sigma_e^2 \cos^2\bar{\theta} + \sigma_n^2 \sin^2\bar{\theta} + 2\sigma_{en}\cos\bar{\theta}\sin\bar{\theta}, \tag{9}$$

$$\sigma_v^2 = \sigma_e^2 \sin^2\bar{\theta} + \sigma_n^2 \cos^2\bar{\theta} - 2\sigma_{en}\cos\bar{\theta}\sin\bar{\theta}, \tag{10}$$

where σ_e^2 and σ_n^2 are, respectively, the unbiased estimate of the variances of the east–west and north–south velocity components (Weber, 1998). Eqs. (9) and (10) were used in this paper to compute the variances of the longitudinal and lateral velocity fluctuations, as well as to estimate their interrelationships.

4. Results and discussion

In this section, we show some results to demonstrate our argument that the Gram–Charlier series can be used more satisfactorily than the Gaussian. The data were selected randomly from our calculations without any pre-judgements.

Probability distribution of the longitudinal velocity fluctuations is shown in Fig. 2, together with the two models used in this paper. In this figure, the 60 min data

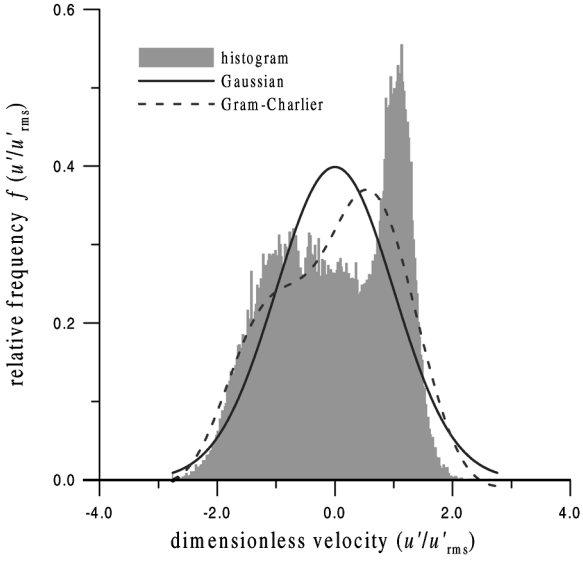

Fig. 2. Distribution of the 60 min longitudinal velocity component, u'. Data measured on 15 August 1998 from 12:00 noon to 01:00 p.m.

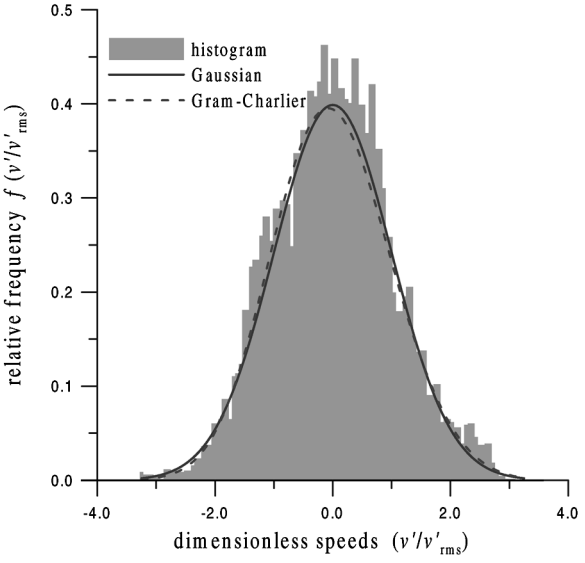

Fig. 3. Distribution of the 60 min lateral velocity component, v'. Data measured on 15 August 1998 from 12:00 noon to 01:00 p.m.

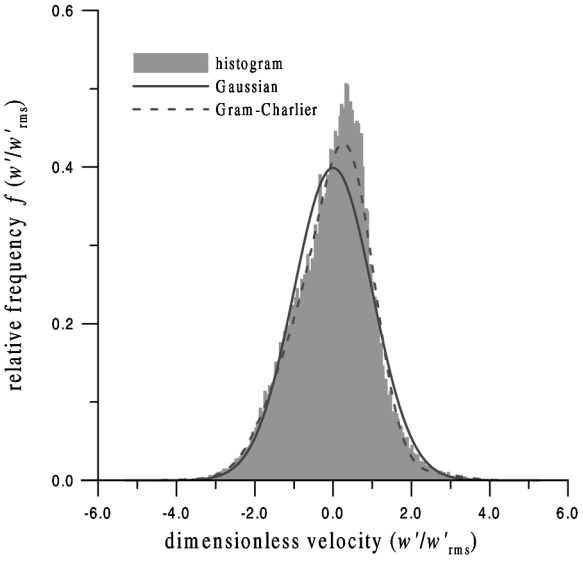

Fig. 4. Distribution of the 60 min vertical velocity component, w'. Data measured on 15 August 1998 from 12:00 noon to 01:00 p.m.

set as a whole was used. The data were recorded on 15 August 1998 for the time period from 12:00 noon to 01:00 p.m. As can be seen from this figure, strictly speaking, none of the statistical models applied can be used to describe the distribution of this particular data set. A large portion of the velocity components are seen to have values larger than their root-mean-square (RMS) value, and this has caused the whole dimensionless data set to be skewed toward left. However, the curve due to the Gram–Charlier series expansion does model the trend of the distribution correctly. Note also that this curve has negative values on both sides of the horizontal axis.

Fig. 3 is the result of fitting the lateral fluctuating components with the two distribution models. The same data set as that of Fig. 2 was used. This time, the distribution is a little skewed toward right, which is truthfully reflected by the Gram–Charlier series. Shown in Fig. 4 is the distribution of the vertical velocity fluctuations. As can be seen, although not as skewed as the other two components, the most part of this velocity is larger than the RMS value, which causes the histogram to have a tail on the left-hand side, and thus also deviates from normality.

As mentioned earlier, the 60 min data were also divided into six 10 min sub-sections to study their statistical properties. The distributions of the three velocity components measured, respectively, on August 15, 25 and 5, at different daytimes were shown in Figs. 5–7. It can be seen from these figures that, irrespectively of the daytime, the distributions of all the three velocity components are better described by the Gram–Charlier series

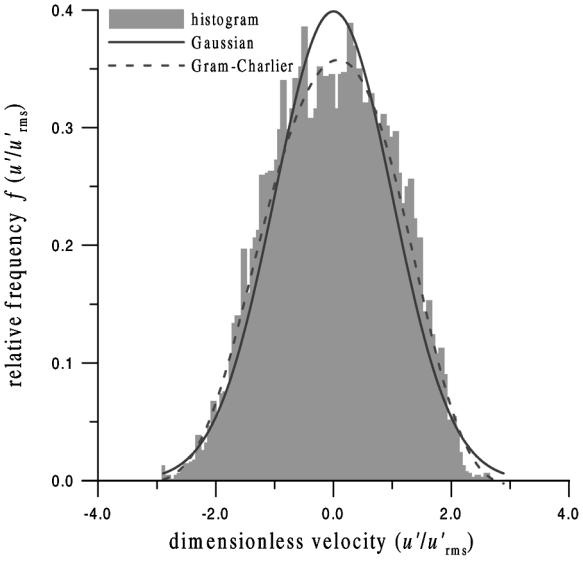

Fig. 5. Distribution of the longitudinal velocity component, u'. Data measured on 15 August 1998 at 12:00 noon. Only 10 min data were used (12:21–12:30 noon).

expansion than by the Gaussian model. The percentages of the data set for the month August 1998, that have satisfied the 90% confidence interval criterion of the Kolmogorov–Smirnov goodness-of-fit test, are tabulated in Table 1. The results for the 60 min whole data set, as well as those divided in 10 min sub-sections are listed. It is seen from Table 1, the Gram–Charlier series expansion fits the data better.

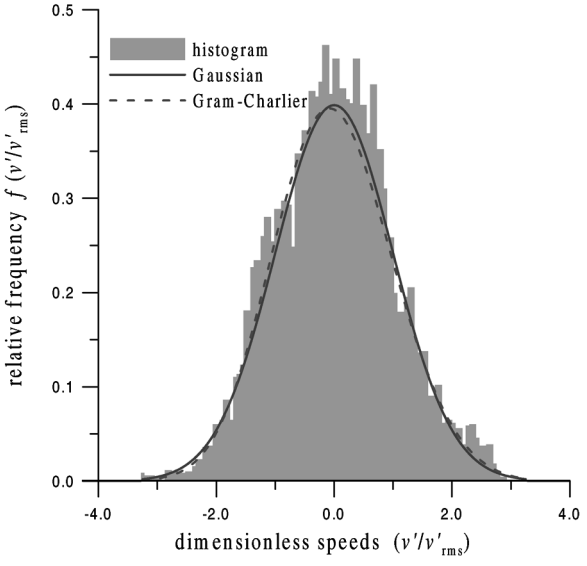

Fig. 6. Distribution of the lateral velocity component, v'. Data measured on 25 August 1998 at 03:00 a.m. Only 10 min data were used (03:31–03:40 a.m.).

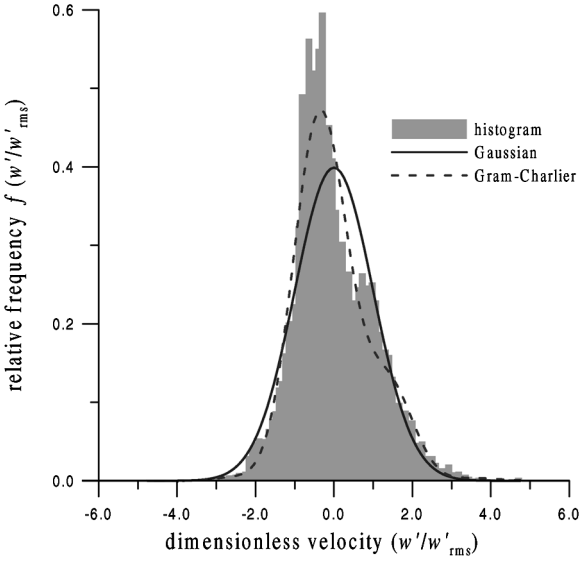

Fig. 7. Distribution of the 10 min vertical velocity component, w'. Data measured on 05 August 1998 at 20:00 (from 20:11 to 20:20).

Knowledge of the underlying statistical properties of a data set can also be acquired by examining the values of the skewness and kurtosis of the data set. Defining the mth central moments as:

$$\mu_m = E(x - \mu_1')^m, \tag{11}$$

where μ_1' is the mean, the mth central moment of a sample set is defined through:

$$m_m = \frac{\sum_{i=1}^{N}(x_i - \bar{x})^m}{N}, \tag{12}$$

where $\bar{x}$ is the mean of the data. The third and fourth moments about the mean are, respectively, the skewness and kurtosis. They can be estimated through (Hahn and Shapiro, 1967):

$$\sqrt{b_1} = \frac{m_3}{\sqrt[3]{m_2}}, \tag{13}$$

$$b_2 = \frac{m_4}{m_2^2}, \tag{14}$$

when the underlying distribution is normal, one would have $\sqrt{b_1} \approx 0$ and $b_2 \approx 3$. The averaged values of the skewness and kurtosis of the wind speed data for the month August 1998 are given in Table 2. It is clear from Table 2 that all the three velocity components have values for the kurtosis that are larger than the normal distribution, i.e., they all are more peaked than the normal distribution. It is also seen that, on the average, the two horizontal velocity components are skewed toward left.

In studying and modelling of pollutant dispersion in the atmosphere, it is important to know the relations between the variances of the velocity components. In the past, several empirical formulae have been proposed by researchers to model these relations. A review concerning the merits and demerits of the respective formulae was given recently by Weber (1998). Among all these models, Weber found that the isotropic Gaussian model (IGM) was the most satisfactory one for his data set. The variances of the longitudinal and the lateral velocity components are assumed to be equal in the IGM, i.e., $\sigma_v \approx \sigma_u$. In Figs. 8 and 9 we show the scatter plots of, respectively, the two paired components $\sigma_u - \sigma_v$, and $\sigma_u - \sigma_w$. Note that these are the transformed values according to Eqs. (8)–(10). However, as can be seen from Figs. 8 and 9, our results, unlike those used by Weber, indicate that a relationship between these two horizontal components of the form

$$\sigma_v \approx 0.745\sigma_u + 0.293 \tag{15}$$

and the following relationship between the variances of the vertical and the longitudinal velocity components, σ_w and σ_u:

$$\sigma_w \approx 0.425\sigma_u + 0.004. \tag{16}$$

Sockel (1984) pointed out that according to the study of Counihan (1975), the following relationships should hold for the variances of the velocity components:

$$\sigma_{v'(30)} \approx 0.75\sigma_{u'(30)} \tag{17}$$

Table 1
Percentage of the records which satisfy the criterion of 90% confidence interval of the Kolmogorov–Smirnov goodness-of-fit tests[a]

Components Sub-set	u'		v'		w'	
	G–C	Gaussian	G–C	Gaussian	G–C	Gaussian
0	42.20	5.05	39.67	4.31	46.06	2.53
1	60.80	11.87	55.04	11.13	67.80	23.89
2	58.87	12.97	55.74	9.84	69.30	26.23
3	58.06	12.54	57.31	10.90	72.09	25.67
4	60.84	13.75	56.80	9.72	71.00	25.56
5	57.73	11.68	58.53	10.63	71.26	24.55
6	58.50	14.13	58.65	11.73	72.78	25.41

[a]G–C represents Gram–Charlier series expansions. Case studied: 01–31 August 1998. The numbers of sub-sets have the following meaning: 0: data of the whole hour (60 min); 1–6: data of each consecutive 10 min (1 = 0–10; 2 = 11–20 min etc.).

Table 2
Averaged values of kurtosis and skewness of the three velocity components for the month of August 1988[a]

Components nth data set	u'		v'		w'	
	Kurtosis	Skewness	Kurtosis	Skewness	Kurtosis	Skewness
0	3.33	− 0.11	3.32	− 0.17	4.39	0.09
1	3.35	− 0.10	3.31	− 0.12	3.99	0.04
2	3.33	− 0.11	3.31	− 0.14	3.94	0.04
3	3.31	− 0.07	3.32	− 0.09	3.99	0.06
4	3.32	− 0.10	3.25	− 0.13	3.98	0.05
5	3.37	− 0.10	3.28	− 0.10	3.97	0.02
6	3.34	− 0.10	3.35	− 0.10	3.99	0.05

[a]The numbers associated with data sets have the same meaning as Table 1.

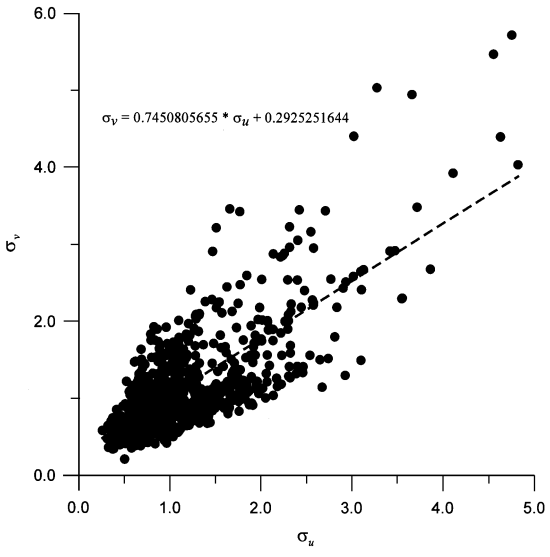

Fig. 8. Scatter plot of the standard deviations of the longitudinal and lateral velocity components. Data obtained for 01–31 August 1998.

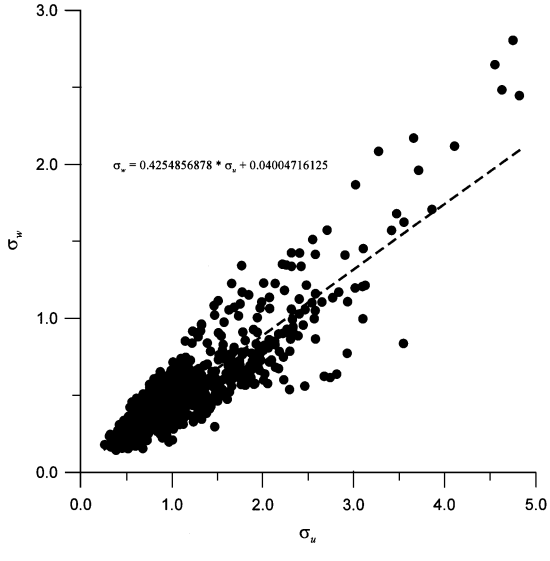

Fig. 9. Comparison of the standard deviations of the longitudinal and vertical velocity components. Data obtained for 01–31 August 1998.

and

$$\sigma_{w'(30)} \approx 0.5\sigma_{u'(30)}, \tag{18}$$

where $u'_{i(30)}$ are the velocity fluctuations measured at 30 m height. Remembering that the height of our anemometer is 26 m, it is seen that our results are comparable with that of Counihan (1975).

5. Discussion and conclusion

A long-term study of the wind field characteristics in Keelung, Taiwan was launched in the late May 1998. The three fluctuating components of winds were collected continuously with a relatively high sampling rate. In this paper, we present the results of our analyses for wind speed data measured in August 1998. Only the statistical distributions of the three velocity components are discussed here. It was found that:

- The probability distributions of the three fluctuating velocity components are to be better described by the Gram–Charlier series expansions, than by the Gaussian model. Adopting the terminology from water wave theory, this fact has the meaning that the velocity fields are subjected to the effects of weakly nonlinearity. Due to enhanced crests and flatter troughs, the probability of the surface fluctuations for nonlinear surface waves is always skewed toward the right. However, our present results seem to indicate that the probabilities for the three fluctuating velocity components do not have any preferable direction for the skewness. The overall values indicate that the majority of the two horizontal velocity components are skewed toward left.
- The standard deviations of the two fluctuating horizontal velocity components do not satisfy the isotropic Gaussian model, in which they are assumed to be equal. Our results indicate that, our σ_vs have magnitudes that are approximately only $\frac{3}{4}$ of their longitudinal counterparts. The magnitude of the standard deviations of the vertical velocity component is approximately half that of the longitudinal component. These results are in agreement with those found by Counihan in 1975.

Acknowledgements

The paper is partly supported by the National Science Council, ROC. Contract No. NSC-87-2611-E-019-035. The authors deeply appreciate all the research associates who have participated in the measurements, as well as the maintenance of the instrument. The authors wish to express their special thanks to Dr. J.-G. Lin for the useful discussions while preparing the manuscript.

References

Bendat, J.S., Piersol, A.G., 1986. Random data. Analysis and Measurement procedures, 2nd Edition. Wiley, New York.

Cook, N.J., 1985. The Designer's Guide to Wind Loading of Building Structures. Buttereorths, London.

Counihan, J., 1975. Adiabatic atmospheric boundary layers: a review and analysis of data from the period 1880–1972. Atmospheric Environment 9, 871–905.

Hahn, G.J., Shapiro, S.S., 1967. Statistical Models in Engineering. Wiley, New York.

Huang, N.E., Long, S.R., 1980. An experimental study of the surface elevation probability distribution and statistics of wind generated waves. Journal of Fluid Mechanics 101, 179–200.

Longuet–Higgins, M.S., 1963. The effect of non-linearities on statistical distributions in the theory of sea waves. Journal of Fluid Mechanics 17, 459–480.

Ochi, M.K., 1992. Applied Probability and Stochastic Processes in Engineering and Physical Sciences. Wiley, Singapore.

Simiu, E., Scanlan, R.H., 1996. Wind Effects on Structures: Fundamentals and Applications to Design, 3rd Edition. Wiley, New York.

Singh, S., Fulker, M.J., Marshall, G., 1994. A wind-tunnel examination of the variation of sigma *y* and sigma *z* with selected parameters. Atmospheric Environment 28, 1837–1848.

Smith, S.D., Anderson, R.J., Oost, W.A., Kraan, C., Maat, N., DeCosmo, J., Katsaros, K.B., Davidson, K.L., Bumke, K., Hasse, L., Chadwick, H.M., 1992. Sea surface wind stress and drag coefficients: the HEXOS results. Boundary-Layer Meteorology 60, 109–142.

Sockel, H., 1984. Aerodynamik der Bauwerke (Aerodynamic of the buildings). Friedrich Vieweg und Sohn, Braunschweig (in German).

Thiebaux, H.J., 1994. Statistical Data Analysis for Ocean and Atmospheric Sciences. Academic Press, San Diego.

Weber, R.O., 1998. Estimators for the standard deviations of lateral, longitudinal and vertical wind components. Atmospheric Environment 32, 3639–3646.